

ME306

MACHINE DESIGN – 1

**PROJECT REPORT – PUMA 560**

BY

GROUP 2

# TEAM

Name	Roll Number	Work
Abhishek Nair	210003005	<ol style="list-style-type: none"> <li>Robot Manufacturing and Assembly along with electronics &amp; set up of Rx Tx for manual control.</li> <li>Integration of end effector to main design</li> <li>Literature review for structural analysis of robot</li> </ol>
Aditya Suwalka	210003008	<ol style="list-style-type: none"> <li>Load analysis( static loading and torque analysis of motors)</li> <li>Forward and inverse kinematics calculations, and verification using IIT KGP software</li> <li>Preliminary assembly of robot</li> </ol>
Akshit Raizada	210003009	<ol style="list-style-type: none"> <li>3D printing</li> <li>WeBots simulation setup and coding for kinematics verification</li> <li>Literature review for fatigue analysis.</li> </ol>
Atharva Dhore	210003018	<ol style="list-style-type: none"> <li>Design of robot along with motor housing</li> <li>Hand Calculations regarding number of cycles and factor of safety</li> <li>Fatigue Analysis Hand Calculations</li> </ol>
Avani Wanjari	210003020	<ol style="list-style-type: none"> <li>Procuring inventory</li> <li>3D printing</li> <li>Fabrication and assembly, ensuring structural integrity and aesthetics.</li> </ol>
Divyam Pandey	210003030	<ol style="list-style-type: none"> <li>Design of robot and servo housing.</li> <li>Manufacturing – 3D printing</li> <li>Assembly &amp; Fabrication</li> </ol>
Harshit Kumar Singh	210003036	<ol style="list-style-type: none"> <li>Preliminary Design</li> <li>Manufacturing of robot</li> <li>Hand calculations for fatigue loading</li> </ol>
Jugal Shah	210003040	<ol style="list-style-type: none"> <li>Static Analysis Hand calculations</li> <li>COMSOL Analysis</li> <li>3D printing</li> </ol>
Monil Pitilya	210003048	<ol style="list-style-type: none"> <li>Static analysis hand calculations</li> <li>3D printing</li> <li>Report compilation</li> </ol>
Tejal Uplenchwar	210003078	<ol style="list-style-type: none"> <li>Design of end effector CAD and its fabrication</li> <li>Manufacturing and assembly of robot</li> <li>Circuit Design for robot – Circuit Diagram on TinkerCAD</li> </ol>

# *Design, Analysis and Manufacture of PUMA 560 robot prototype*

## **Introduction**

This report delves into the design and structural analysis of the PUMA 560 robotic arm, highlighting its mechanical architecture, kinematics, and dynamics. Developed by the Unimation Company in the 1980s, the PUMA 560 is renowned for its six degrees of freedom, versatility, and robust construction. Advancements in materials, manufacturing, and control systems have further enhanced its capabilities. The investigation examines design considerations, structural components, actuation mechanisms, and control architecture to understand operational efficacy. Additionally, kinematic analysis reveals motion capabilities and trajectory planning, while structural analysis evaluates mechanical integrity and dynamic response under varying loads, ensuring stability and safety. This report provides a comprehensive overview of the PUMA 560 robotic arm.

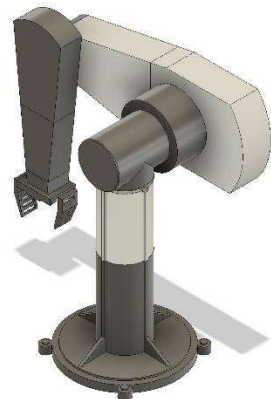
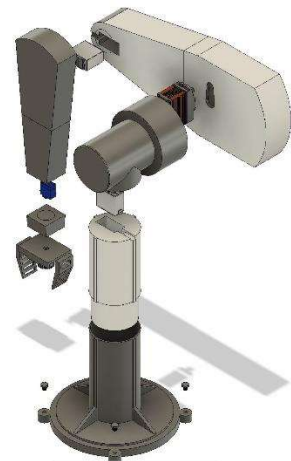
## **Design**

### Main Links:

In designing the robot from scratch, we initially referenced standard dimensions and then scaled it down to create a tabletop version. With four revolute joint connections (excluding the end effector joints), accommodating four servo motors of varying specifications posed a challenge. To address this, we utilized a negative extrusion of the servo motor and a connection fin on the two links to be joined, facilitating easy servo mounting. Departing from the original model where the waist rotation motor was mounted at the base with power transmitted via gears, we opted to mount the motor at the revolute joint to simplify power transmission and save time. To ensure stability, the robot was equipped with a robust base featuring fastener holes for secure grounding. All joints were constructed using the interference fit principle to circumvent issues related to fastener availability.

### End Effector:

The effector was specifically engineered to fit onto Link 3 of the main body, ensuring a cohesive assembly. It incorporates a dual rack and pinion mechanism to enable precise claw motion, thereby enhancing gripping capabilities. Dimensioning of the model was carefully conducted, considering factors such as the gripping area and the required width between the gripper arms. This meticulous approach ensures optimal functionality and compatibility with the intended tasks, facilitating efficient and reliable operation of the robotic arm.



## Manufacturing and Assembly

We utilized PLA (Polylactic Acid) for 3D printing throughout the manufacturing process of the robotic arm. Here's a breakdown of the printing specifications for each component:

### Base:

The base of the robotic arm serves as its foundation, providing stability and support for the entire structure. It was designed and 3D printed with a 10% infill, ensuring a balance between strength and weight. Additionally, a negative extrusion was incorporated into the design to seamlessly accommodate servo motors, facilitating the first degree of freedom. To enhance durability and reinforcement, mild steel rod was inserted from the base link to Link 1.

### Link 1:

Mounted onto the base, this component was printed with a 10% infill. This, too, has a negative extrusion to accommodate the servo motor, providing 2nd degree of freedom. A mild steel rod was inserted from the base link to link-1 to provide extra reinforcement.

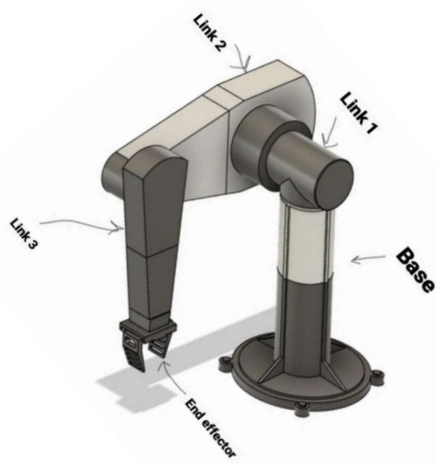


Fig-1: Nomenclature of Links

### Link 2:

This part was printed in two segments. The first segment, unfortunately, was printed with a higher-than-intended 50% infill due to a printing error. Reprinting wasn't feasible due to material constraints. The second segment was printed with a 5% infill.

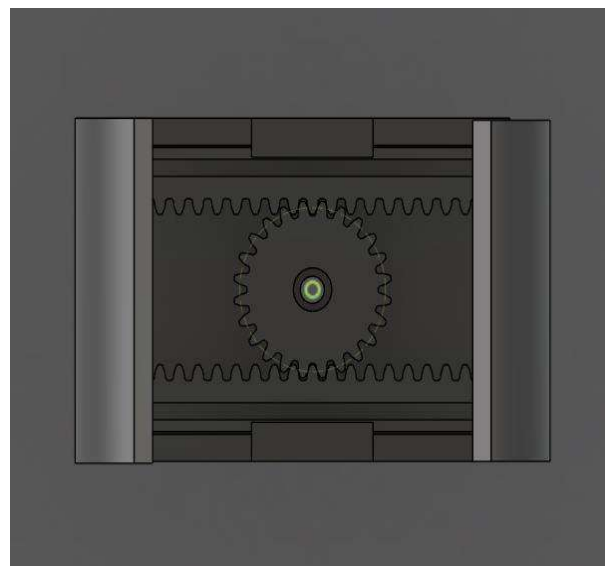
Due to the inadvertent imbalance in torque caused by the differing infill percentages of Link 2, there was a noticeable strain on Link 1. To rectify this issue, weights were strategically added to the other end of Link 1, effectively balancing the torques and ensuring smoother operation of the robotic arm.

### Link 3:

Link 3 was printed with a 5% infill. It was printed in 2 parts due to space constraints of the 3D printer.

### End Effector:

It was printed with 5% infill. A rack and pinion mechanism was used to make the end effector. To actuate it, a Sg90 servo motor is used to rotate the gear.



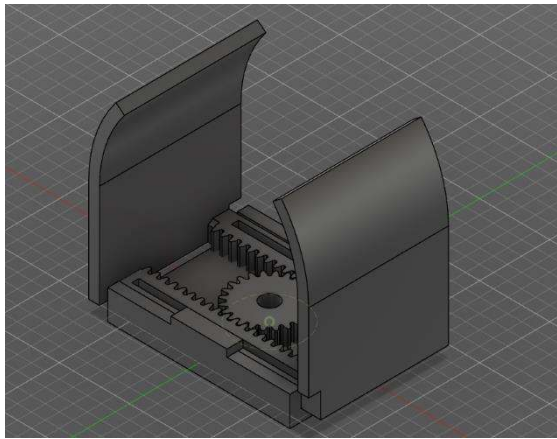
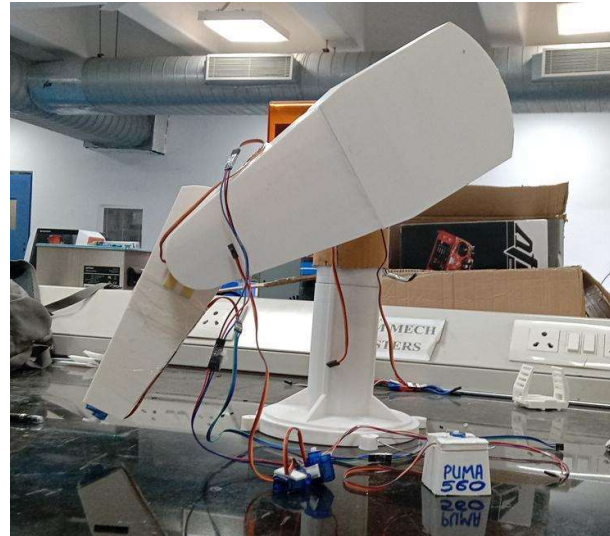
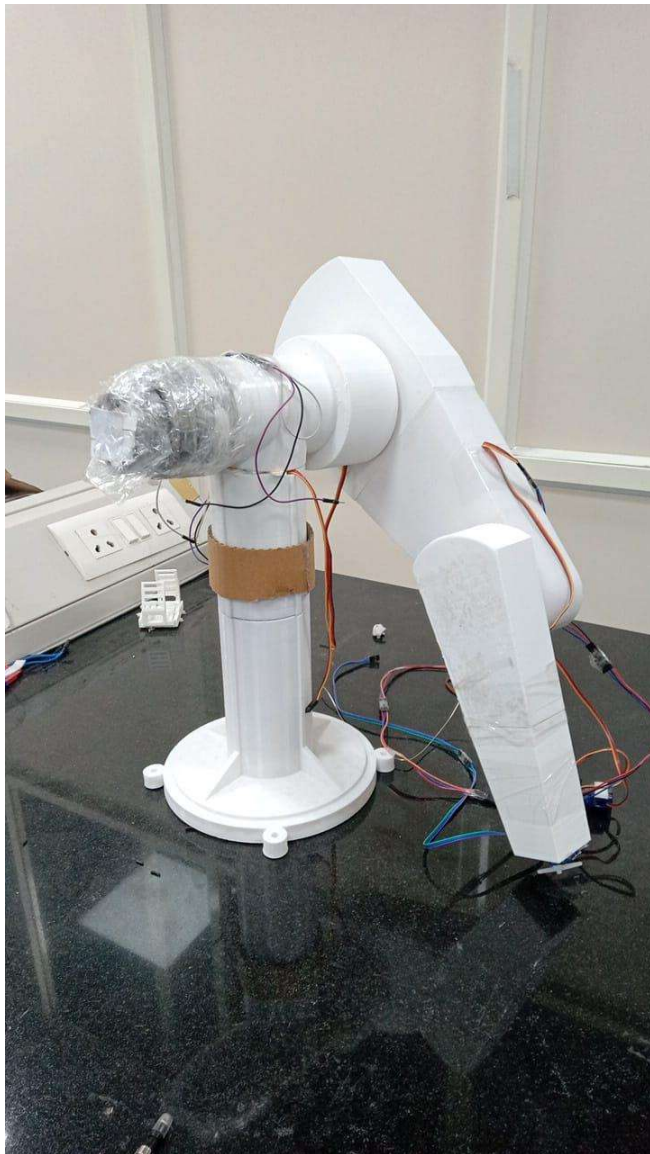
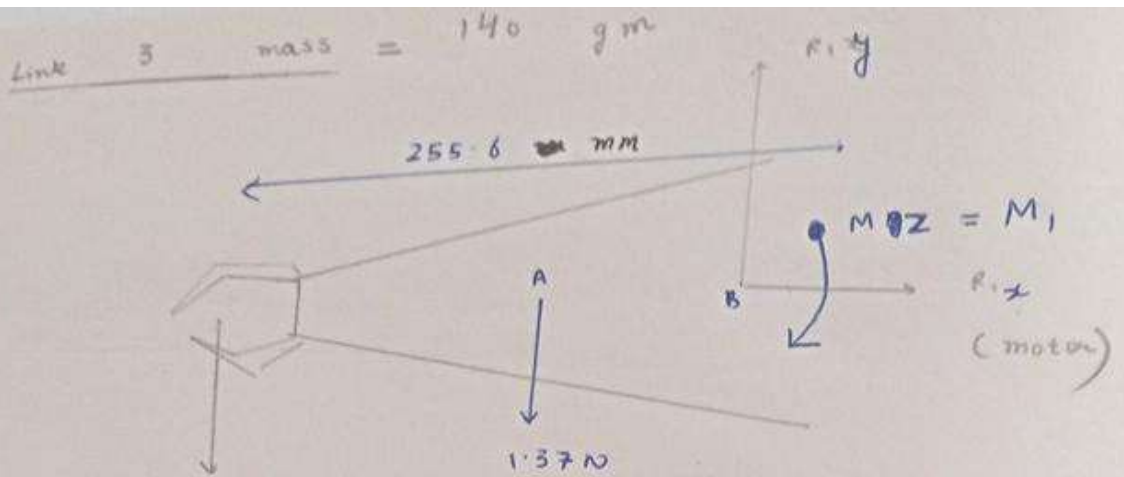


Fig-2,3: CAD of End Effector



### Initial Load and Torque Analysis

Hand calculations were performed to validate the accuracy of the CAD model and to determine the necessary specifications for the servos required at each link of the robot. These calculations involved assessing the forces and torques exerted on each link during operation. By meticulously analyzing these factors, suitable servos were selected to ensure they could effectively handle the mechanical demands placed on them. This rigorous process helped guarantee the reliability and performance of the robotic arm, aligning its physical capabilities with the intended design specifications.



(Holding mass)  $\rightarrow 1 \text{ kg} + 50 \text{ gm}$   
 $1 \times 9.81 + 0.4905 \text{ N}$

$\approx (98.1 \text{ N})$

+ it has zero  
<sup>also</sup> negligible mass)

→ Maximum torque of

$M G 996 R$   
 11

$0.981 \text{ N-m} = 10 \text{ kg-f-cm}$  out  
 5 Vals.

( taken by Arduino Forum)

$R_{zx}$   
 $R_{zy}$   
 $M_z$

given by motor  
 so that we can  
 hold over object at  
 the particular  
 position.

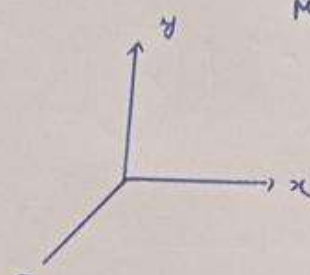
For simplifications; we have taken  
 horizontal position

$R_{xy}$

$M_{yz} = M_1$

$R_{zx}$   
 (motor)

$M_z =$  Torque  
 about z  
 axis



Weight of end effector =  $50 \text{ gm} \times 9.81$   
 Force it will give (gravity) =  $490.5 = 50 \text{ gm} \times$   
 $= 0.4905 \text{ N}$

Assumptions →

- ① Assuming link of same cross-section throughout the length
- ② gravity force acting on centre of mass of ~~base~~ link.

$$\text{Force at com (A)} = 0.14 \text{ kg} \times 9.81 \\ = 1.3734 \text{ N}$$

Statically balanced in that position

(i) Moment about ~~OB~~

$$\text{Req } M_Z = 9.81 \times 255.6 \text{ (mm)} + 1.37 \times \frac{255.6}{2}$$

$$(M_i) = 2.68 \text{ N-m}$$

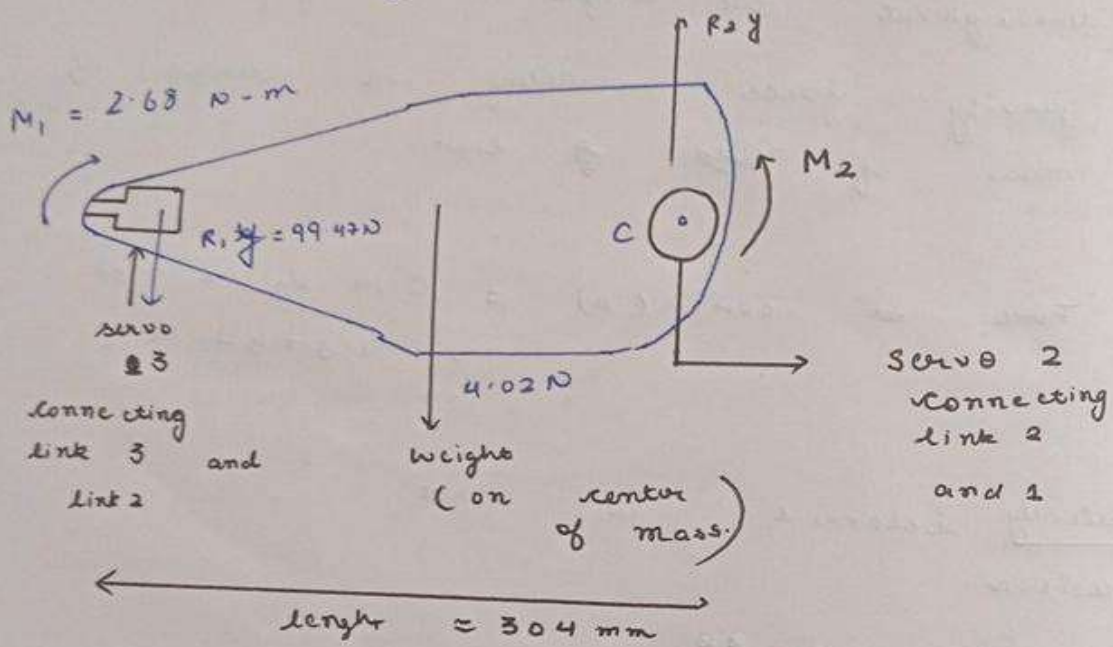
(ii)  $R_{1x} = 0$  (Force balance in  $x$ -direction)

$$(iii) R_{1y} = 99.47 \text{ N}$$

Hence, we specified motor (MG 996R)  
not able to lift 1 kg  
force material.

Having using servo of 20 kg - f cm we can hold maximum of 800 gm max

Link - 2  $\rightarrow$  IN HORIZONTAL POSITION  
(~~statically~~ balanced)



Weight of link around = 410 gm

Now; Moment about C.

$$99.47 \times 304 \text{ mm} + 4.02 \times 152 = M_2$$

$$M_2 = 30.84 \text{ N-m}$$

High torque motors such as servo motors are required to lift 1 kg block.

## Finite Element Analysis – Static Loading

### Assumptions:

- 1) Links are rectangular and have a uniform cross-section.
- 2) All the links are in one line, and the loads are not eccentric.
- 3) No stress concentrations are considered.

From the hand calculations mentioned after this section, we got a rough estimation of the maximum von Mises stress in links 1 and 2, which is now used to validate the FEA results in COMSOL Multiphysics.

### COMSOL - Multiphysics tool Results

### Link 2:

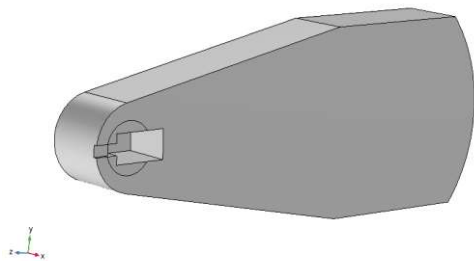


Fig-7

### Link 3:

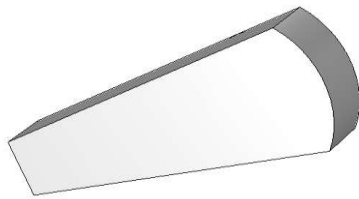


Fig-4

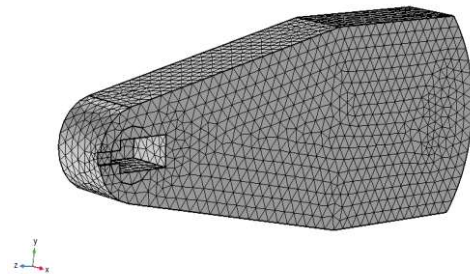


Fig-8

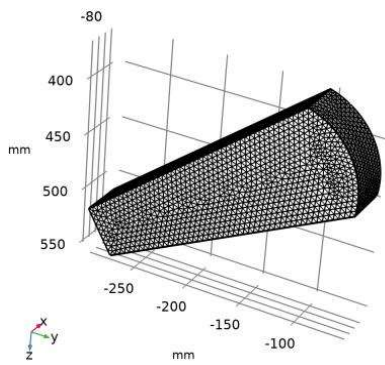


Fig-5

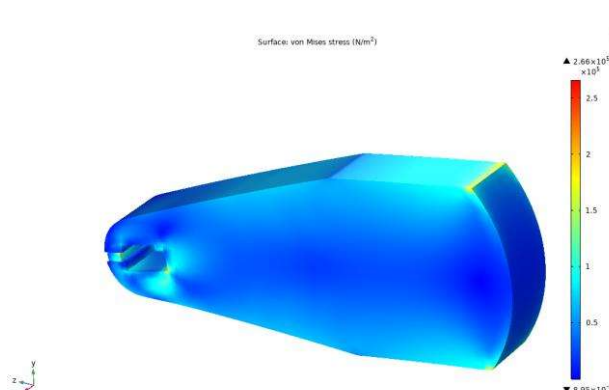


Fig-9

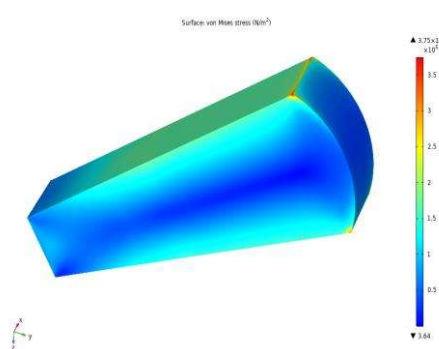


Fig-6

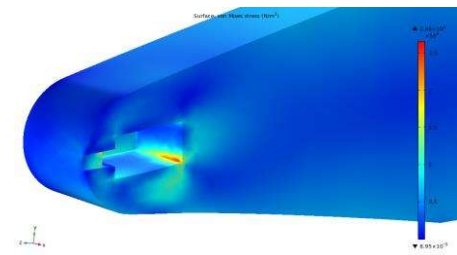


Fig-9

The above contours show that the calculated and FEA values are in the 5% error region, thus validating our FEA Model in COMSOL Multiphysics. Also, the above contour shows the areas of stress concentration.

Once the results for two simple geometry links were validated, we did FEA for our base link and link 3.

The complex internal geometry of the base, link 1, and FEA contours are shown below.

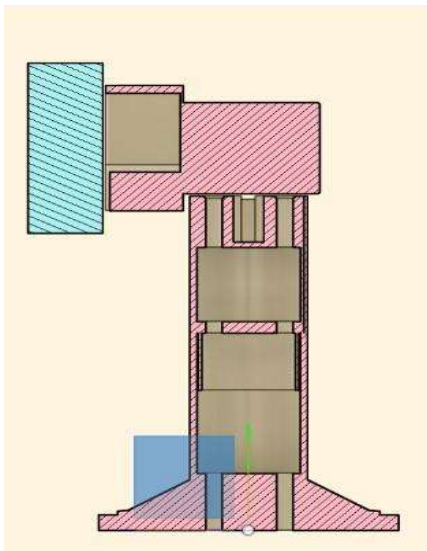


Fig-10:

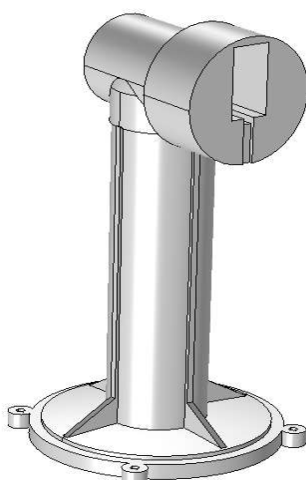


Fig-11

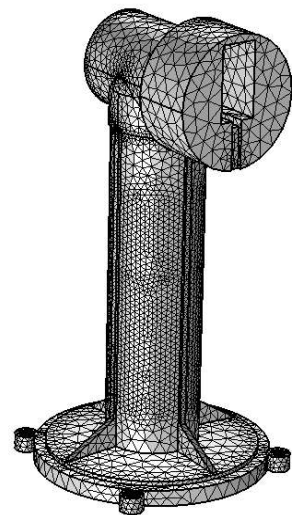


Fig-12

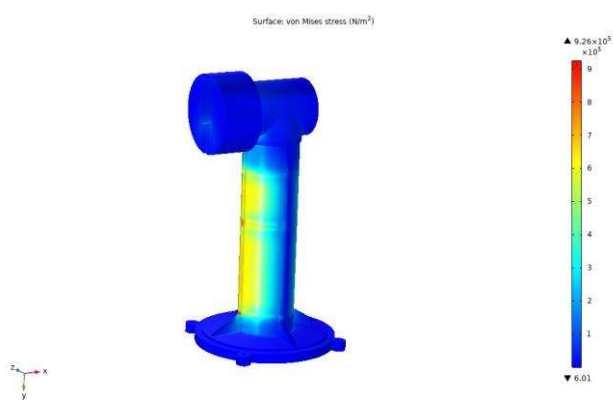


Fig-13

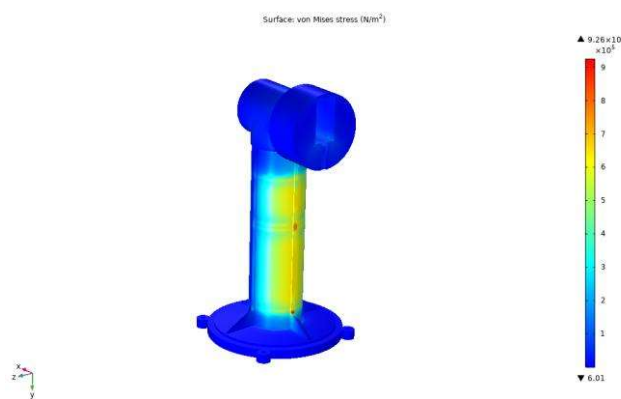


Fig-14

We designed the PUMA 560 robotic arm, calculated its loads and stresses, performed the FEA analysis, and finalized the design according to the values deformations and maximum stresses acting on it on applying a particular load. We were also able to validate the FEA results with our hand calculations.

## Hand Calculations for validating FEA

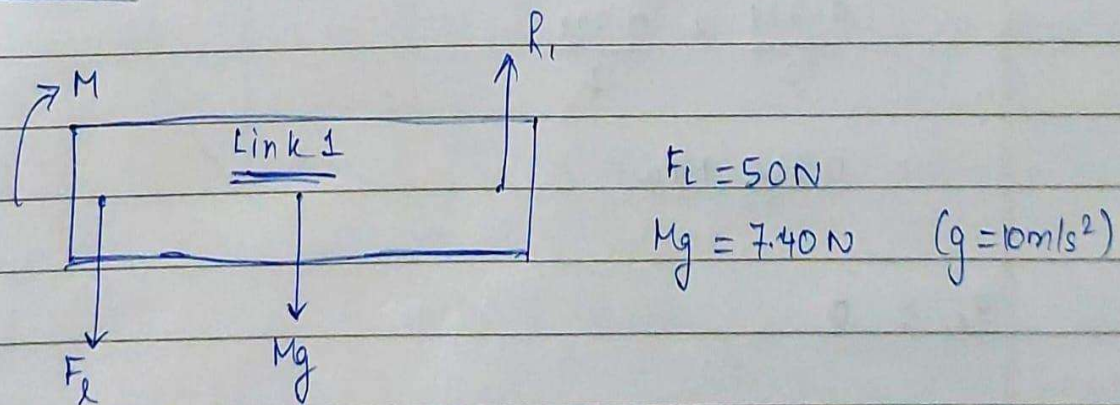
Given :

Link 1  $\rightarrow$   $l = 0.25\text{m}$ , Mass of Link 1 :  $740\text{g}$   
 $b = 0.07\text{m}$   
 $h = 0.05\text{m}$

$$F_L = 50\text{N}$$

Link 2  $\rightarrow$   $l = 0.3\text{m}$ , Mass of Link 2 :  $2.512\text{kg}$   
 $b = 0.15\text{m}$   
 $h = 0.05\text{m}$

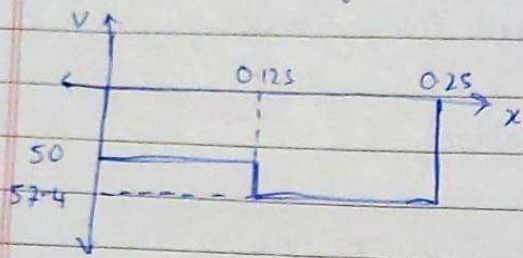
Calculation :



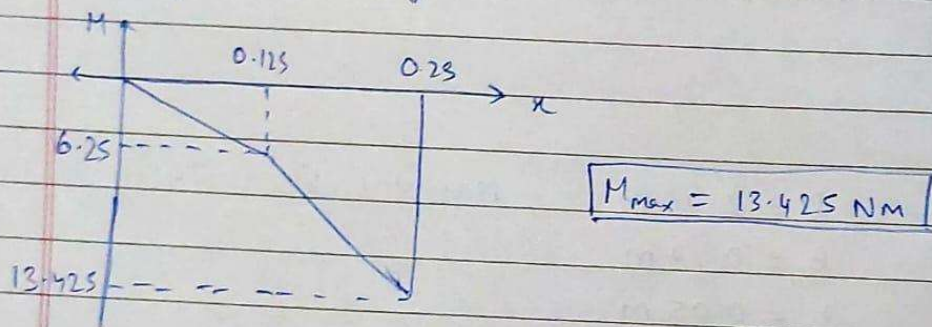
$$R_1 = F_L + Mg$$

$$R_1 = 57.40\text{N}$$

Shear Moment diagram,



Bending Moment diagram,



$$M_{\max} = 13.425 \text{ NM}$$

$$\sigma = \frac{13.425 \times 0.07 \times 6}{0.05 \times (0.07)^3}$$

$$\sigma_{\max} = 0.328 \text{ MPa}$$

$$\begin{aligned}\sigma_1 &= \frac{\sigma_x + \sigma_y}{2} + \sqrt{\left(\frac{\sigma_x - \sigma_y}{2}\right)^2 + \tau^2} \\ &= \frac{0.328}{2} + \frac{0.328}{2} \\ &= 0.328 \text{ MPa}\end{aligned}$$

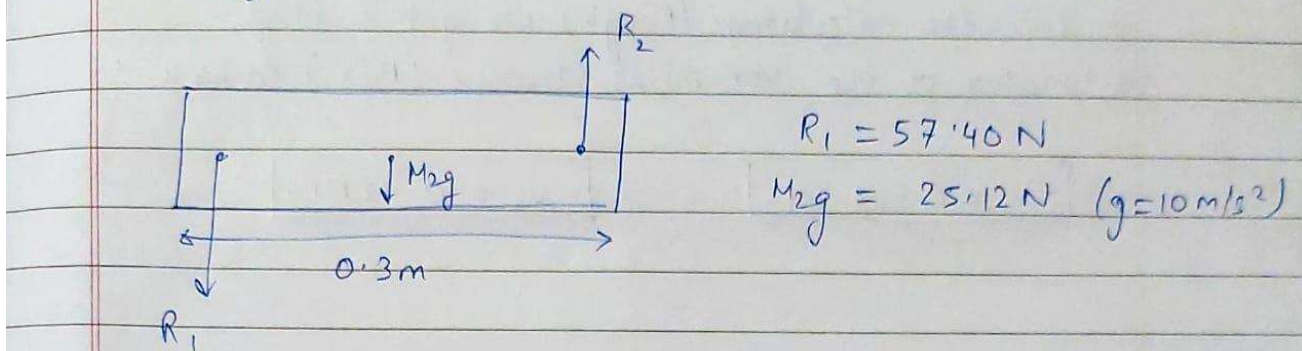
$$\sigma_2 = 0$$

$$\text{So, } \sigma_v = \sqrt{\sigma_1^2 + \sigma_2^2 - \sigma_1 \sigma_2}$$

$$= \sigma_1$$

$$\sigma_v = 0.328 \text{ MPa}$$

→ Similarly for Link 2,



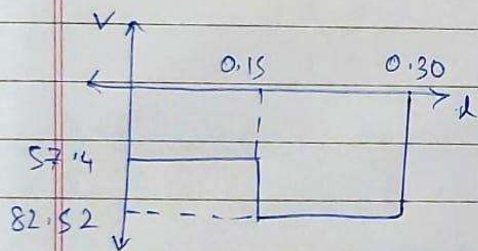
$$R_1 = 57.40 \text{ N}$$

$$M_{2g} = 25.12 \text{ N} \quad (g = 10 \text{ m/s}^2)$$

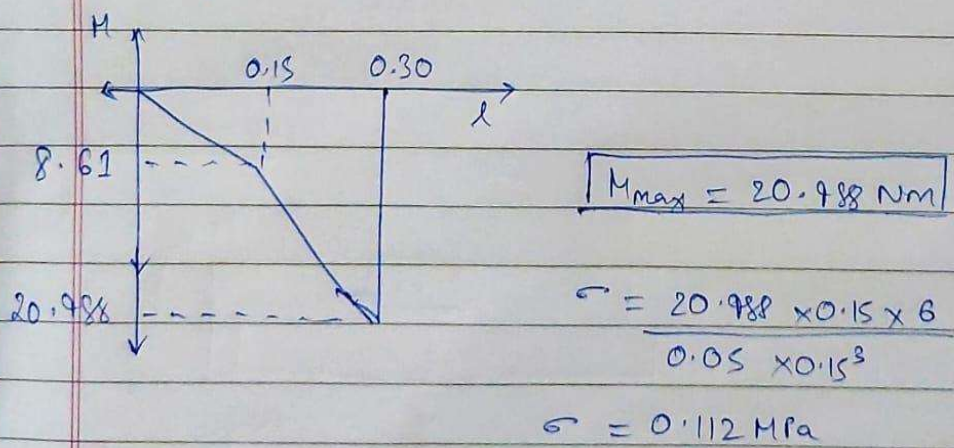
$$R_2 = R_1 + M_{2g}$$

$$R_2 = 82.52 \text{ N}$$

Shear moment diagram,



Bending Moment diagram,



$$\therefore \sigma_v = 0.112 \text{ MPa}$$

## Fatigue Loading Hand Calculations

Note: Infill is taken as 100%.

Values for endurance strength are the same as the maximum von mises stress. This is done because the results obtained in the following research paper:

<https://www.sciencedirect.com/science/article/pii/S2452321618300076>

suggest that the values do not change very much based on the type of loading and maximum von mises stress can be taken safely.

$$\log \frac{\sigma_{\max}}{\sigma_{UTS}} = -\frac{1}{k} \log N + \log a, \quad k = 5.4$$

For  $\log a$ ,

$$\log 1 = -\frac{1}{5.4} \log 10 + \log a$$

$$\log a = \frac{1}{5.4}$$

$$\therefore \log \left( \frac{\sigma_{\max}}{\sigma_{UTS}} \right) = -\frac{1}{5.4} (\log N - 1)$$

$$\Rightarrow \log N = 1 - 5.4 \log \left( \frac{\sigma_{\max}}{\sigma_{UTS}} \right) \quad \text{①}$$

$$\sigma_{UTS} = 33 \text{ MPa}$$

For link 1,

$$\sigma_{\max} = \sigma_v = 0.328 \text{ MPa}$$

From eq ①,

$$\log N = 1 - 5.4 \log \left( \frac{0.328}{33} \right)$$

$$\Rightarrow N = 6.52 \times 10^{11}$$

$\therefore N \approx 10^{11}$  cycles to failure

For link 2,

$$\sigma_{\max} = \sigma_v = 0.112 \text{ MPa} \quad (\text{From hand calculations})$$

Similarly using eq ①,

we found  $N \approx 10^{16}$  cycles to failure

if we take  $\sigma_{\max} = 0.266 \text{ MPa}$  (From simulation)

$N \approx 10^{12}$  cycles to failure

For base

$$\sigma_{\max} = \sigma_v = 0.926 \text{ MPa}$$

$N \approx 2 \cdot 10^9$  cycles to failure

## Forward & Inverse Kinematics

Forward and inverse kinematics are concepts commonly used in robotics, computer animation, and biomechanics to describe the relationship between the positions, orientations, and movements of different parts of a system.

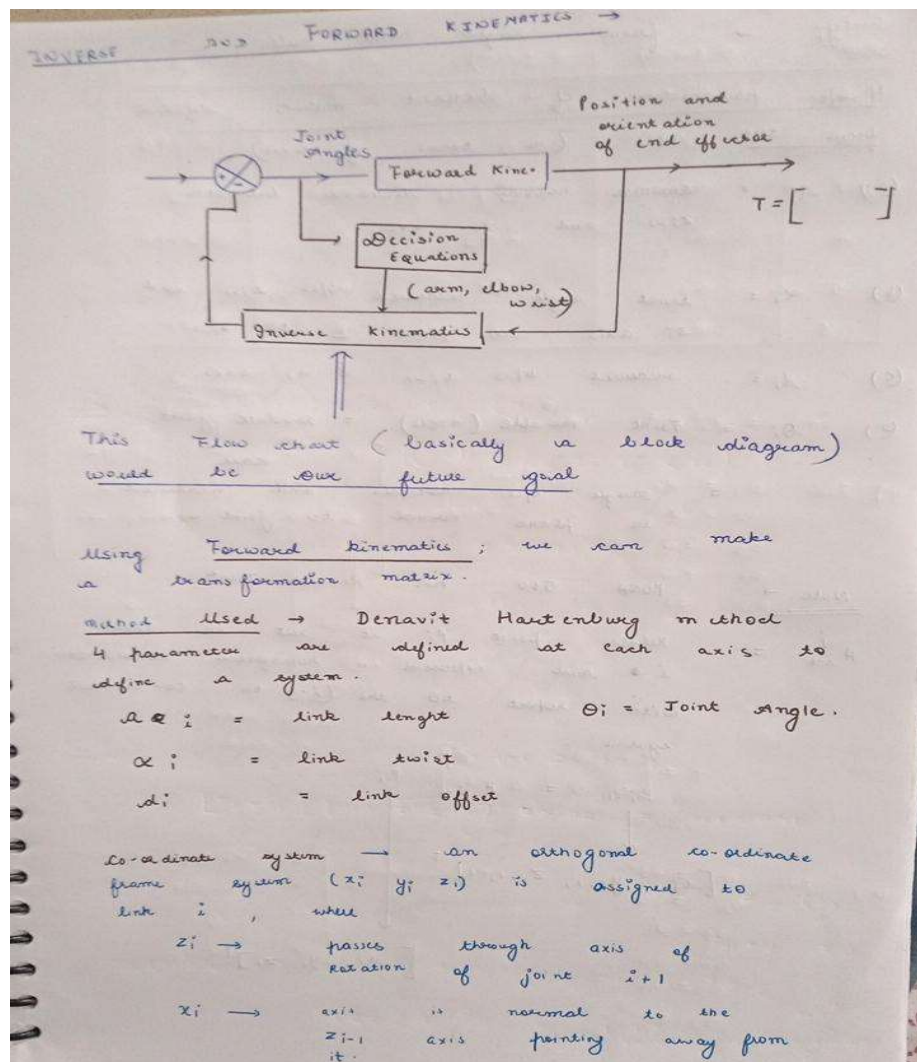
### Forward Kinematics:

Forward kinematics deals with predicting the position and orientation of an end-effector (like a robot's hand or a character's limb) given the joint angles or lengths of a robot's segments. In simpler terms, it's about determining where the end of a robotic arm will be when you set specific angles for each joint. This process involves applying a series of transformations, typically using matrices in 3D space, to calculate the end position based on the joint variables.

### Inverse Kinematics:

Inverse kinematics, on the other hand, involves working backward from a desired end-effector position to determine the joint configurations that will achieve that position. This is often more complex than forward kinematics, as it may involve solving nonlinear equations or using numerical methods to find solutions. Inverse kinematics is particularly useful in robotics when you want to control the end-effector of a robot arm to reach a specific point in space, allowing you to calculate the joint angles needed to achieve that position.

### **Hand Calculations:**



$y_i \rightarrow$  from right hand rule

4 imp parameters of Denavit matrix, defined from the axis (in terms of axis)

(a)  $a_i$  = common normal distance between  $z_{i-1}$  and  $z_i$  axes.

(b)  $\alpha_i$  = twist angle measured b/w  $z_{i-1}$  and  $z_i$  axis in plane  $\perp$  to  $a_i$

(c)  $d_i$  = measured b/w  $x_{i-1}$  &  $z_i$  axes

(d)  $\theta_i$  = Joint variable (angle) = revolute joint in our case

= single b/w normals and measured normal to joint axis.

Note  $\rightarrow$  PUMA 560 has Revolute Joint

$A_{i-1}^j$  = Relative point  $P_i$  at rest in link  $i \bullet$  and expressed in homogeneous co-ordinates with respect to the  $(i-1)$  th co-ordinate system

$$P_{i-1} = A_{i-1}^j P_i$$

$$[x_{i-1}, y_{i-1}, z_{i-1}, 1]^T$$

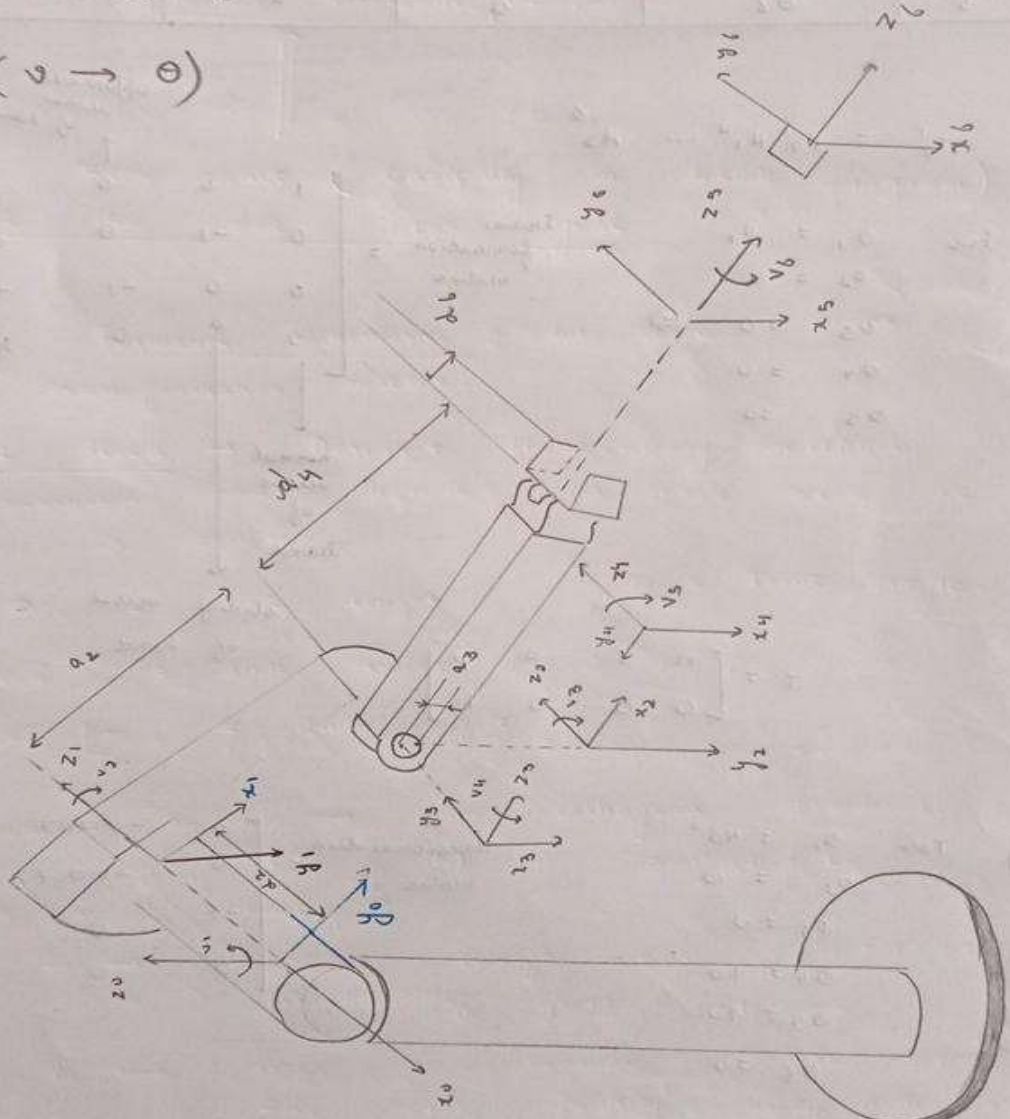
$$[x_i, y_i, z_i]^T$$

$$P_{i-1}^i = \begin{bmatrix} \cos \theta_i & -\sin \theta_i \sin \alpha_i & \sin \alpha_i \sin \theta_i & a_i \cos \theta_i \\ \sin \theta_i & \cos \alpha_i \cos \theta_i & -\sin \alpha_i \cos \theta_i & a_i \sin \theta_i \\ 0 & \sin \alpha_i & \cos \alpha_i & 0 \\ 0 & 0 & 0 & 1 \end{bmatrix}$$

for a rotatory joint

$v \rightarrow$  Equivalent to  $\theta$

$(v \rightarrow \theta)$



Joint no. i	$\theta_i$ (rad)	$\alpha_i$ (rad)	$r_{ai}$ (m)	$d_i$ (m)
1	$\theta_1$	$-90^\circ / \pi/2$	0	0
2	$\theta_2$	0	0.304	0.156
3	$\theta_3$	$90^\circ / \pi/2$	0.0010	0
4	$\theta_4$	$-\pi/2$	0	0.2556
5	$\theta_5$	$\pi/2$	0	0
6	$\theta_6$	0	0	0.061

$$T_0^1 = A_0^1 A_1^2 \dots A_5^6$$

(i) For  $\theta_1 = 0^\circ$   
 $\theta_2 = 0$   
 $\theta_3 = 0 \Rightarrow$   
 $\theta_4 = 0$   
 $\theta_5 = 0$

Transformation matrix = 
$$\begin{bmatrix} 1 & 0 & 0 & 0.42 \\ 0 & -1 & 0 & 0.12 \\ 0 & 0 & -1 & -0.41 \\ 0 & 0 & 0 & 1.0 \end{bmatrix}$$

↑  
 normal vector of hand  
 ↓  
 sliding vector of hand  
 ↑  
 approach vector of hand  
 ↓  
 position vector of hand

$$T = \begin{bmatrix} n & s & a & p \\ 0 & 0 & 0 & 1 \end{bmatrix}$$

(ii) For  $\theta_1 = 45^\circ$   
 $\theta_2 = 0$   
 $\theta_3 = 0$   
 $\theta_4 = 90^\circ$   
 $\theta_5 = 90^\circ$   
 $\theta_6 = 0$

Transformation matrix = 
$$\begin{bmatrix} 0 & -0.707 & -0.707 & 0.2 \\ 0 & -0.707 & 0.707 & 0.42 \\ -1 & 0 & 0 & -0.41 \\ 0 & 0 & 0 & 1 \end{bmatrix}$$

Angles to avoid self-collision  
 (in degrees)

$$\begin{aligned} j_1 &= 160^\circ \text{ to } 160^\circ \\ j_2 &= -225^\circ \text{ to } 45^\circ \\ j_3 &= 225^\circ \text{ to } -45^\circ \\ j_4 &= 170^\circ \text{ to } -110^\circ \\ j_6 &= 266^\circ \text{ to } -226^\circ \end{aligned}$$

also verified  
 by

- ① Webots Sim
- ② IIT KGP Software

## Forward kinematic solution of PUMA 560 using ITKGP software:

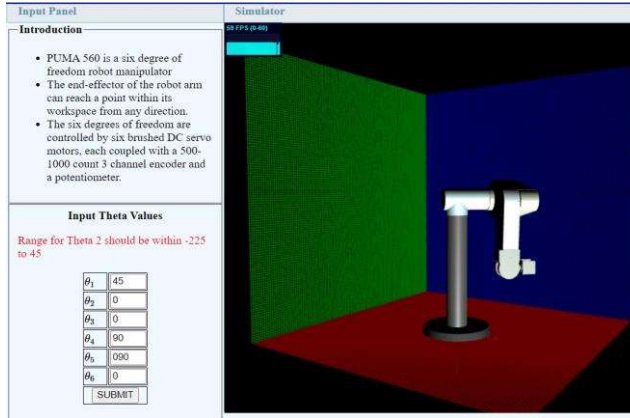


Fig-15

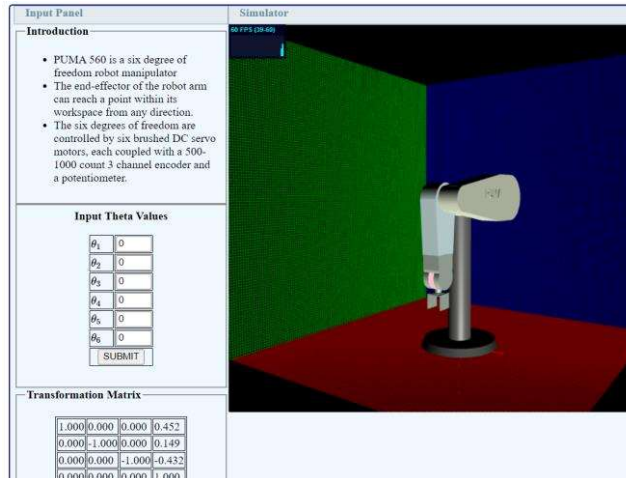


Fig-16

### Inverse kinematics Calculations:

For the PUMA 560 robot manipulator, we are given the DH model T06 which contains the orientation (rotation matrix) and the position (displacement matrix) of the end-effector. The angles at each joint is determined by decoupling the PUMA 560 robot manipulator. We initially solve the position ( $P_{5x}$ ,  $P_{5y}$ ,  $P_{5z}$ ) of the frame 5 and use these coordinate values to determine the angles ( $\theta_1$ ,  $\theta_2$ ,  $\theta_3$ ) at the first three joints.

We start by determining the position of frame 5 as shown in Figure 1. That is-

$$P_5 = \begin{bmatrix} P_x - d_6 a_x \\ P_y - d_6 a_y \\ P_z - d_6 a_z \end{bmatrix}. \quad (1)$$

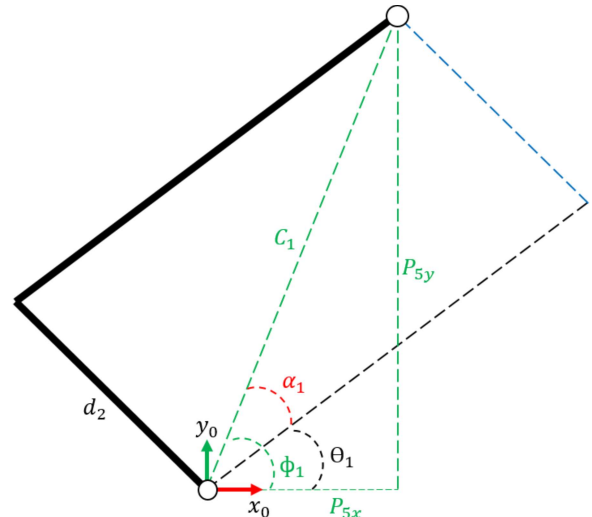


Fig-17: x0 – y0 plane (Top View)

Next, we solve the angles at the first three joints by viewing PUMA 560 robot manipulator movement across  $x_0 - y_0$  and  $x_0 - z_0$  planes. In Figure 2, the joint angle  $\theta_1$  is defined by the difference between angles  $\phi_1$  and  $\alpha_1$ .

The angle  $\alpha_1$  is defined as-

$$\alpha_1 = \arcsin\left(\frac{d_2}{C_1}\right) \quad (2)$$

Where,

$$C_1 = \sqrt{P_{5x}^2 + P_{5y}^2}$$

Equation (2) can be expressed in terms of atan2 function. We define

$$D_1 = \frac{d_2}{\sqrt{P_{5x}^2 + P_{5y}^2}}$$

and yield

$$\alpha_1 = \text{atan2}(D_1, \sqrt{1 - D_1^2}) \quad (3)$$

The angle  $\phi_1$  is defined as

$$\phi_1 = \text{atan2}(P_{5y}, P_{5x}) \quad (4)$$

The joint angle  $\theta_1$  is derived as

$$\theta_1 = \text{atan2}(P_{5y}, P_{5x}) - \text{atan2}(D_1, \sqrt{1 - D_1^2}) \quad (5)$$

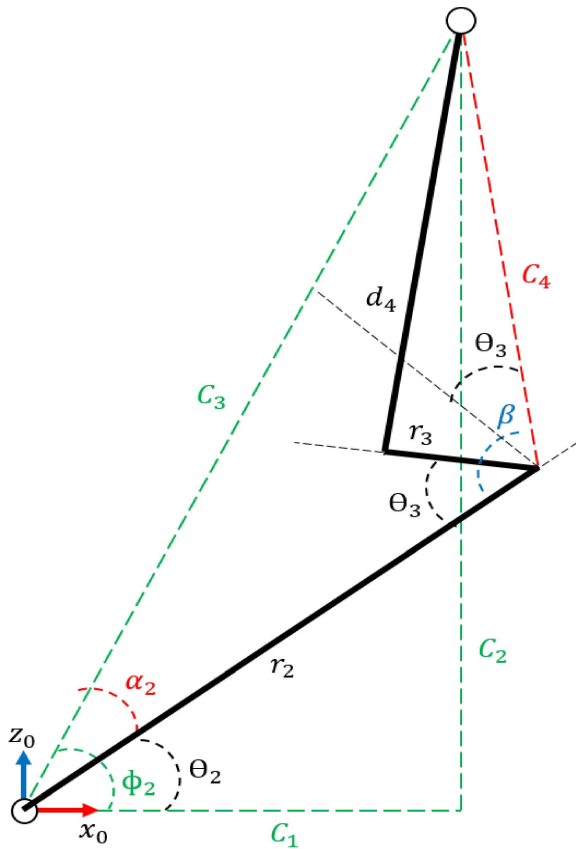


Fig-18: x0 – z0 plane (Side View)

We derived the equations to solve for the joint angles  $\theta_1$  and  $\theta_2$ . We define the distances

$$C_2 = P_{5x} - d_1 \quad (6)$$

$$C_3 = \sqrt{C_1^2 + C_2^2} \quad (7)$$

$$C_4 = \sqrt{r_3^2 + d_4^2} \quad (8)$$

and apply cosine law to determine angles,  $\alpha_2$  and  $\beta$ . We get the equations

$$\cos \alpha_2 = \frac{C_3^2 + r_2^2 - C_4^2}{2r_2C_3} \quad (9)$$

and

$$\cos \beta = \frac{C_2^2 + r_2^2 - C_3^2}{2r_2C_2} \quad (10)$$

that gives the cosine value of  $\alpha$  and  $\beta$ . We set

$$D_2 = \frac{C_3^2 + r_2^2 - C_4^2}{2r_2C_3}$$

and

$$D_3 = \frac{C_2^2 + r_2^2 - C_3^2}{2r_2C_2}$$

to define

$$\alpha_2 = \text{atan2}\left(\sqrt{1 - D_2^2}, D_2\right) \quad (11)$$

and

$$\beta = \text{atan2}\left(\sqrt{1 - D_3^2}, D_3\right). \quad (12)$$

The angle  $\phi_2$  is determined by

$$\phi_2 = \text{atan2}(C_2, C_1). \quad (13)$$

The joint angle  $\theta_2$  is the difference between angles  $\phi_2$  and  $\alpha_2$  as shown in Figure 3. That is

$$\theta_2 = \text{atan2}(C_2, C_1) - \text{atan2}\left(\sqrt{1 - D_2^2}, D_2\right). \quad (14)$$

For the joint angle  $\theta_3$ , we have

$$\theta_3 = \text{atan2}\left(\sqrt{1 - D_3^2}, D_3\right) - 90. \quad (15)$$

After we obtained the angles at the first three joints, we used the angles to solve for the forward kinematics for frame 0 to frame 3. We solve the homogeneous transformation matrix  $T_{36}$  for frame 3 to frame 6 by taking the dot product between  $T_{06}$  and the inverse of  $T_{03}$ . In general, DH model for 6 degrees of freedom manipulator is defined as

$$T_6^0 = T_1^0 \cdot T_2^1 \cdot T_3^2 \cdot T_4^3 \cdot T_5^4 \cdot T_6^5. \quad (16)$$

We can simplify the model to  $T_{06} = T_{03}T_{36}$  and define

$$T_6^3 = T_3^0 \cdot [T_6^3]^{-1}. \quad (17)$$

The angles at joint 4 to 6 is determined by deriving a set of equations from the homogeneous transformation matrix  $T_{36}$ . The rotation matrix  $R_{36}$  holds the orientation of the end-effector in reference to frame 3. That is

$$R_6^3 = \begin{bmatrix} c\theta_4c\theta_5c\theta_6 - s\theta_4s\theta_6 & c\theta_4c\theta_5s\theta_6 - c\theta_6s\theta_4 & c\theta_4s\theta_5 \\ c\theta_4s\theta_6 + c\theta_5c\theta_6s\theta_4 & c\theta_4c\theta_6 + c\theta_5s\theta_4s\theta_6 & s\theta_4s\theta_5 \\ -c\theta_6s\theta_5 & s\theta_5s\theta_6 & c\theta_5 \end{bmatrix} \quad (18)$$

where the notation,  $s\theta = \sin \theta$  and  $\cos\theta = \cos \theta$ , is adapted. The  $R_{36}$  is a component in the homogeneous transformation matrix  $T_{36}$ . We derived the joint angles  $\theta_4$ ,  $\theta_5$  and  $\theta_6$  by equating the numerical values of  $T_{36}$  in equation (26).

We obtain the joint angle  $\theta_4$  by

$$\frac{\sin \theta_4 \sin \theta_5}{\cos \theta_4 \sin \theta_5} = \frac{T_6^3(2, 3)}{T_6^3(1, 3)}. \quad (19)$$

The joint angle  $\theta_4$  is defined as

$$\theta_4 = \text{atan2}\left(T_6^3(2, 3), T_6^3(1, 3)\right). \quad (20)$$

For joint angle  $\theta_5$ , we have  $\cos \theta_5 = T_6^3(3, 3)$  and use this equation to find  $\theta_5$  in terms of  $\text{atan2}$  function. The joint  $\theta_5$  is defined as

$$\theta_5 = \text{atan2}\left(\sqrt{1 - T_6^3(3, 3)^2}, T_6^3(3, 3)\right). \quad (21)$$

Lastly, the joint angle  $\theta_6$  is derived by

$$\frac{\sin \theta_5 \sin \theta_6}{-\cos \theta_6 \sin \theta_5} = \frac{T_6^3(3, 2)}{T_6^3(3, 1)}. \quad (22)$$

We have the joint angle  $\theta_6$  as

$$\theta_6 = \text{atan2}\left(T_6^3(3, 2), -T_6^3(3, 1)\right). \quad (23)$$

## Simulation

Robotic systems, especially those involving moving parts and heavy machinery like the PUMA 560 robotic arm, pose inherent safety risks during testing and development. Webots mitigates these risks by providing a virtual platform where you can experiment with different control algorithms and scenarios without endangering personnel or equipment.

This section outlines the key aspects of our simulation, demonstrating how it validates and complements the results obtained in previous sections, including failure and stress analysis, kinematics calculations, and design justifications.

### Simulation Setup:

In our Webots simulation, we faithfully replicated the warehouse environment, complete with conveyor belts conveying products and shelves for storing them. The PUMA 560 robotic arm was integrated into this environment, positioned strategically to pick up these products from the conveyor belt and place them onto designated shelves.

An ultrasonic distance sensor was attached to the PUMA 560 to detect if the products were in the grabbing range of the robot. The robot also verified our forward and inverse kinematic calculations as we confirmed that the calculated joint angles and end-effector positions accurately

reflected the expected behavior of the robot in the simulated environment.

Such a simulation is essential for estimating important metrics like max joint angle to avoid self-collision, cycle time and important edge cases, which can be tested without damage to the commercial robot.

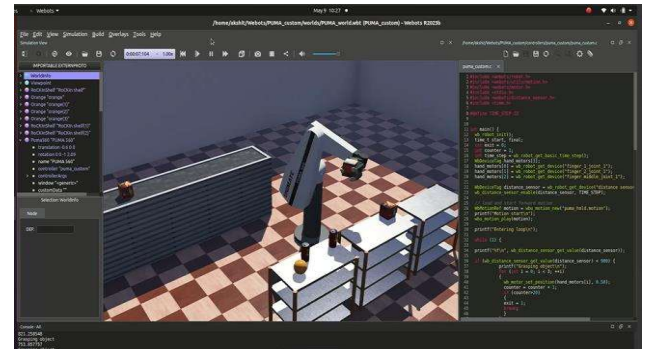


Fig-19

Method = 3 bar open chain kinematics

Cycle Time = 9 seconds

Max joint angles to avoid self-collision:-

j1 -> -160 to 160 degrees

j2 -> -225 to 45 degrees

j3 -> 225 to -45 degrees

j4 -> 170 to -110 degrees

j5 -> 100 to -100 degrees

j6 -> 266 to -266 degrees

## Hardware and Electronics

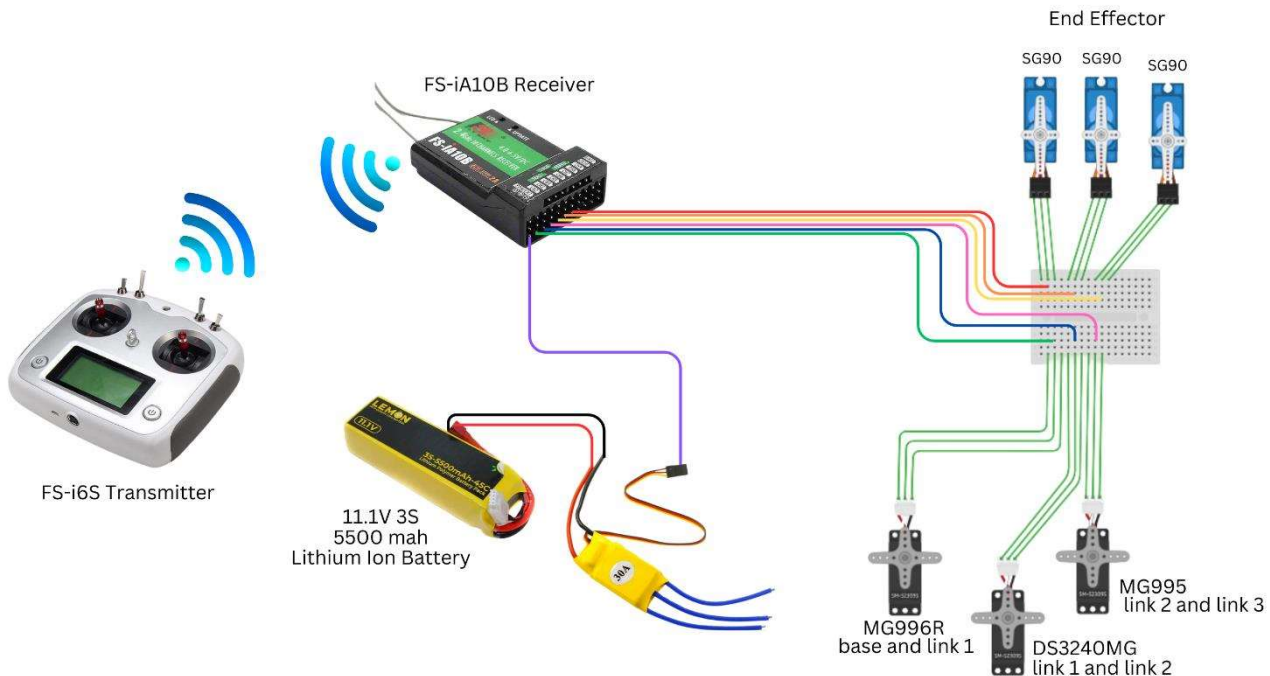
The robot's actuation employed a variety of servo motors tailored to different functions. To connect the base link and the first link, we utilized the *MG996R*, a high-torque servo motor capable of 360-degree rotation. Link-1 to Link-2 connection was facilitated by the *DS3240MG*, a metal gear servo offering 180-degree movement. Link-2 to Link-3 was managed by the *MG995*, a 180-degree plastic gear servo motor.

For achieving the three degrees of freedom in the end effector, we employed three *SG90* servo motors, chosen for their suitability despite lower torque. Control signals were transmitted via Rx-Tx communication, with a *Flysky FS-i6S 2.4GHz 10CH AFHDS 2A RC Transmitter* paired with an *FS-iA10B 10CH Receiver*. The receiver's six channels were utilized to command the six servos effectively.

Powering the receiver and all six servo motors was managed by an electronic speed controller,

drawing power from a reliable *Lemon 5500mAh 3S 45C/90C Lithium Polymer Battery Pack* via a 30A ESC. This setup ensured smooth and precise control over the robot's movements.

## Circuit Diagram



## Future Work

- 1) Enhancing the Joints between links by using longer servo shafts
- 2) Better Weight Balancing
- 3) Using more reinforcement inside the 3D printed components.
- 4) Enhanced Gripper design
- 5) Using base mounted motors and gear system rather than servos.